

## ORIGINAL ARTICLE

# Preparation and Administration of a Controlled-Release Delivery System of Chitosan Hydrogel loaded with Methadone and Piroxicam in Experimental Defect of Tibial in Rats; Histopathological Evaluation

Pegah Khosravian<sup>1</sup>, Moosa Javdani<sup>2\*</sup> , Melika Masoudi<sup>2</sup>, Abdolnaser Mohebi<sup>2</sup>, Amin Bigham Sadegh<sup>3</sup>, Abolfazl Barzegar<sup>4</sup>

<sup>1</sup> Medical Plant Research Center, Shahrekord University of Medical Science, Shahrekord, Iran

<sup>2</sup> Department of Clinical Sciences, Faculty of Veterinary Medicine, Shahrekord University, Shahrekord, Iran

<sup>3</sup> Department of Clinical Sciences, Faculty of Veterinary Medicine, Shiraz University, Shiraz, Iran

<sup>4</sup> Department Clinical Sciences, Faculty of Veterinary Medicine, Shahid Chamran University of Ahvaz, Ahvaz, Iran

\*Corresponding Author: Moosa Javdani  
Email: [javdani59@gmail.com](mailto:javdani59@gmail.com)

Received: 18 December 2022 / Accepted: 14 January 2023

## Abstract

**Purpose:** In this study, a controlled-release drug delivery system loaded with piroxicam and methadone was synthesized and used subcutaneously in rats with experimental tibial defect, and healing were assessed histopathologically.

**Materials and Methods:** For this purpose, 100 adult female rats were randomly divided into five equal groups; control group, chitosan group, piroxicam group, methadone group, and piroxicam-methadone group. The morphological structure of the synthesized drug systems was studied by scanning electron microscope. In addition, the structure of the hydrogels was investigated by Fourier transform infrared spectroscopy and while releasing the hydrogels' gelation time, the release of piroxicam and methadone from the hydrogels was evaluated in vitro.

**Results:** Histological results of the 3rd day of the study showed the lowest extent and severity of inflammation in the chitosan, piroxicam, and piroxicam-methadone groups, while on the 7th day, tissue inflammation and the extent of bleeding were lower in the piroxicam, methadone, and piroxicam-methadone groups than in the other groups. Evaluation of new bone formation on day 21 showed that the chitosan, piroxicam, and methadone groups had better repair than the other groups.

**Conclusion:** It seems that in the control group that did not receive any treatment intervention, following the experimental bone defect, the highest inflammatory response was observed in histological examination and finally the weakest bone repair. On the other hand, the presence of piroxicam, methadone, and chitosan in the piroxicam-methadone group (all of which have anti-inflammatory effects) also seems to have a negative effect on the repair.

**Keywords:** Bone Healing; Inflammation; Methadone; Piroxicam; Chitosan.

## 1. Introduction

The bone healing process is biologically intertwined with acute inflammation and the innate immune system. In fact, when the bone is exposed to damage and inflammatory stimuli (trauma, infection, etc.), regular biological processes that occur with the innate immune system are regulated to have a beneficial effect on the local healing of bone. Therefore, if this response is suppressed or chronic, inflammation can be detrimental to repair [1]. Inflammatory cells are the main source of inflammatory signals introduced during the initial phase of bone healing [2]. Inflammatory cells accumulation and their mediators have been shown to play a key role in modulating and not modulating bone healing. In addition, the importance of osteoporotic cells, growth factors, blood flow, and mechanical environments in bone regeneration and successful fracture healing has been well documented [3]. In addition, bone cells, such as osteoblasts and chondrocytes are responsible for releasing inflammatory cytokines within a few days after injury [4].

In other words, a bilateral interaction occurs between inflammation and affects bone cells during fractures, and drug intervention affects each part of the inflammation and the healing process as a whole. However, the administration of Nonsteroidal Anti-Inflammatory Drugs (NSAIDs), as well as opioids, is considered an important treatment for pain management after bone injuries and fractures [5-7]. The importance, advantages, and disadvantages of each of these drugs can be seen in different studies. Despite the high potency of opioids in controlling pain due to the abundance of opioid receptors in the body and the high potential for side effects (including addiction, respiratory suppression, cognitive impairment, emesis, constipation, etc.) following the administration of opioids, the administration of alternative drugs, including NSAIDs is recommended [8]. In addition, the question that arises is whether the administration of any drug with an anti-inflammatory effect can affect or even impair bone repair.

Another concept in modern therapies is the use of controlled-release drug delivery systems to provide a sufficient amount of drugs in a specified period of time. A controlled delivery system can be achieved by releasing hydrogels. This release depends on the physicochemical properties of the polymer structure, the bioactive factor, and the binding density. One of the biodegradable polymers is chitosan, which is a linear

aminopolysaccharide that combines randomly dispersed bonds of D-glucosamine and N-acetyl-D-glucosamine due to its physicochemical and its unique biology has provided many incentives for the scientific and effective development of the drug delivery system [9, 10]. Also, chitosan has been widely focused on as a promising alternative therapy for bone formation [11]. In the descriptive evaluation of tissue sections, Hematoxylin-Eosin (H&E) staining was considered to examine inflammation, necrosis, hemorrhage, and condition of bone cells. Also, in order to prove the process of bone healing on the days of sampling, a histopathological evaluation of the created bone defect was performed.

In the present study, in addition to preparing and evaluating the controlled-release delivery system of chitosan hydrogel loaded with methadone and piroxicam, histological changes were examined after the administration of this system in rats with an experimental defect in the bone.

## 2. Materials and Methods

### 2.1. Preparation of Methadone and Piroxicam-Loaded Chitosan Hydrogel

Methadone and piroxicam were obtained from Iranian pharmaceutical Companies, Daropaksh and Exir, respectively. Low molecular chitosan (CAS No.9012-76-4) - Sigma-Aldrich) and glycerol phosphate disodium hydrate (CAS No.13408-09-8) (GP) were purchased from Sigma-Aldrich Co. (St Louis, MO, USA). Other reagents and solvents were purchased from Merck (Darmstadt, Hesse, Germany). In this part, 480 mg of chitosan was dispersed in 12 ml of 0.1 M acetic acid solution at first. After three hours of stirring, a solution of 120 mg piroxicam and 2 mg methadone in 5 ml water was added to the chitosan hydrogel. In a separate container, 3.2 g of GP was dissolved in 2 ml of deionized water. The chitosan combination and the GP solution were then placed in an ice bath at 4 °C until they reached that temperature. Following that, the GP solution was added dropwise to the chitosan mixture for around 10 minutes before being agitated for another 2 hours [12, 13]. The final manufactured hydrogel as the piroxicam-methadone group was stored at 4 °C for usage in later procedures as a combined chitosan hydrogel.

To prepare chitosan hydrogel or loaded with piroxicam or methadone alone, none, only 120 mg of piroxicam or 2 mg of methadone was added, respectively (Chitosan,

Piroxicam, Methadone groups); however, the amount of water was the same as 5 ml in the duration of hydrogel preparation steps. These systems were designed to provide the appropriate daily dose for every 250 g rat at 7 days (piroxicam 1 mg/kg/day and methadone 2 mg/kg/day).

## 2.2. Characterization

A Scanning Electron Microscope (SEM) was used to investigate morphological properties. The prepared sample was placed in a  $-20^{\circ}\text{C}$  freezer to quickly freeze and then dried with a freezer dryer (CHRIST, Gamma LSC). For SEM analysis, a very thin layer was isolated. SEM (SEM, FEI, Quanta 200) was used to study the morphological structure of the layer. For further examination in SEM analyses, a sample made entirely of chitosan was developed and compared to a cross-linked chitosan hydrogel produced by GP. The structure of hydrogels was investigated using FTIR (Nicolet Magna IR-550, USA). Chitosan, piroxicam, methadone, and piroxicam-methadone samples were used to evaluate and confirm the hydrogel preparation. The duration of gel formation in the produced hydrogel was investigated. To eliminate bubbles, pour 2 ml of the prepared GP chitosan sample into a 5 ml vial and hold for 4 hours at  $4^{\circ}\text{C}$ . The vial was then immersed in a bath (at  $24^{\circ}\text{C}$  and  $37^{\circ}\text{C}$ ) and the hydrogel gel time was measured every minute by placing the vial horizontally. If the solution is totally stable, the gelation time is taken into account. In vitro drug release from produced hydrogels was determined. 1 g of the produced hydrogel was poured in 500 ml of phosphate buffer with a pH of 7.4 at  $37^{\circ}\text{C}$  and shaken at 100 rpm by a microbial shaker incubator (Jal-Tajhiz, JTSL-40 Refrigerated). 1 ml of sample was obtained at a predetermined sampling time, and 1 ml of fresh buffer was replaced. Using the standard curve produced from the phosphate buffer solution at 7.4 pH, the collected samples were analyzed by UV/visible spectrophotometer (Shimadzu, UV-1800) at 323 and 289 nm for piroxicam and methadone, respectively. This test was carried out three times. All the steps of preparation of methadone and piroxicam-loaded chitosan hydrogel were done at the laboratory of medical plant research center, Shahrekord university of medical science, Shahrekord, Iran.

## 2.3. Animals and Experiment Groups

The present study has been approved by the Research Council of the Faculty of Veterinary Medicine at Shahrekord University (1399-08-07). The laboratory animals used for the present study were

female wistar rats weighing 235–255 g, which were kept in a standard environment with free access to water and food. Their feeding was standard with commercial pellets, and in addition, the policy of changing the animal's beds daily was considered to keep the animals' habitats clean and to prevent unwanted diseases and infections. One hundred rats were randomly divided into five equal groups; (A) the control group in which only experimental surgical intervention was performed and they did not receive any pharmacological intervention; (B) the chitosan group received only chitosan hydrogels, (C) the piroxicam group received chitosan hydrogel loaded with piroxicam, (D) the methadone group received chitosan hydrogel loaded with methadone, and (E) the piroxicam-methadone group received chitosan hydrogel loaded with piroxicam and methadone. The creation of the bone defect model was done in the Surgery Section, faculty of veterinary medicine, Shahrekord University, Shahrekord, Iran.

## 2.4. Induction of Experimental Bone Defect

Following general anesthesia of animals using an intraperitoneal injection of a combination of ketamine (80 mg/kg; ketamine 5%; Alfasan) and xylazine (10 mg/kg; xylazine 2%; Alfasan) [14, 15], the proximal region of the right tibia of rats underwent routine surgical preparation. After a 1 cm surgical incision along the skin of the medial surface of the tibial epiphysis, skin, fascia, and underlying muscles were pushed aside and a 2 mm diameter, 2 mm deep hole was made using a low-speed microdrill at the epiphysis of the bone. Finally, after thoroughly washing the surgical site and ensuring that there is no apparent bleeding, in all groups, muscles, fascia, and skin, were sutured with monocryl and nylon routinely. After surgery, in each group, depending on the definition of that group, its controlled-release system was administered subcutaneously. Antibiotics (ampicillin; 25 mg/kg) were administered for 5 days after surgery, and the animal's health was monitored for behavior, food intake, weight, injuries, and stitches at least twice daily. Days 3, 7, and 21 after surgery were included as sampling times in the whole groups.

## 2.5. Histopathological Examinations

In the descriptive evaluation of tissue sections, hematoxylin-eosin (H&E) staining was considered to

examine inflammation, necrosis, hemorrhage, and condition of bone cells. For this purpose, after sacrificing the animals by overdosing with anesthetics, the proximal part of the affected tibia of rats was carefully separated and immersed in 10% formalin, and sent to the histopathology laboratory. After routine processing of tissue specimens and providing of paraffin blocks, serial sections of tissues with a thickness of 5  $\mu\text{m}$  were prepared using a microtome (Leica RM 2055; Nassloch, Germany) and were stained by H&E. Subsequently, the sections were examined by light microscope (Micros Austria, MC100LED, Germany) at 200 $\times$  and 400 $\times$  magnifications.

### 3. Results

#### 3.1. SEM

The morphology of chitosan and crosslinked chitosan hydrogel was studied using an SEM at a magnification of 10  $\mu\text{m}$ . The collected pictures revealed porous scaffolds in both samples. As demonstrated in the data, the pore size in chitosan hydrogel decreases from 10-20  $\mu\text{m}$  to 5-10  $\mu\text{m}$  in crosslinked chitosan hydrogel. The network of crosslinked chitosan hydrogel is more sophisticated than that of chitosan hydrogel. Both of these observations support the idea that GP molecules cross-link chitosan chains (Figure 1).

#### 3.2. FTIR Study

Figure 2 shows the FTIR spectra of chitosan, piroxicam, methadone, and piroxicam-methadone groups. FTIR confirmed the final formulation of the formation of piroxicam-methadone. Figure 2A depicts the composite sample of Chitosan. All the index peaks of ingredients such as chitosan and GP can be seen in this Figure (Figure 2A) as before the study [12]. It can be attributed to the stretching vibration of  $\text{NHCO}$ -,  $\text{PO}_4^-$ , and  $\text{-P-O-C-}$  at 1576, 1058, and 965  $\text{cm}^{-1}$ , respectively, as they can be observed in Figures 2B, 2C, and 2D. In Figure 2B, because of piroxicam existence, stretching vibration of  $\text{sp}^2$  and  $\text{sp}^3$  C-H was found at 2973 and 2934  $\text{cm}^{-1}$ , respectively. 1571  $\text{cm}^{-1}$  and 1402  $\text{cm}^{-1}$  of C=C aromatic ring stretching confirmed the presence of a phenyl ring in the piroxicam structure. The asymmetric and symmetric S=O stretching appeared at 1333 and 1135  $\text{cm}^{-1}$ , respectively. Stretching of orthodisubstituted phenyl was seemed at 759  $\text{cm}^{-1}$ . The peaks at 1677, 1077, and 1047  $\text{cm}^{-1}$  were attributed to C=O, C-O, and C-N stretching, respectively.

In the methadone group, because of the presence of an aromatic ring in methadone as piroxicam, the stretching vibrations of  $\text{sp}^2$  and  $\text{sp}^3$  C-H were observed at 2916 and 2849  $\text{cm}^{-1}$ , respectively (Figure 2C). The phenyl ring in the methadone structure induced C=C aromatic ring stretching at 1618  $\text{cm}^{-1}$  and 1401  $\text{cm}^{-1}$ . Moreover, the stretching peaks of C=O and C-N were observed at 1641 and 1069  $\text{cm}^{-1}$ , respectively.

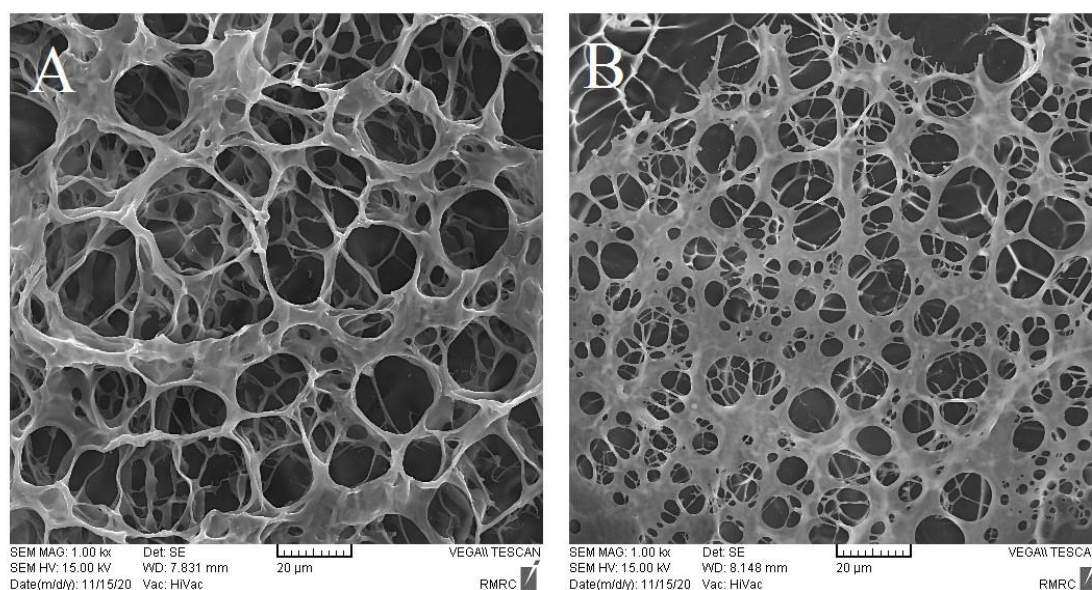
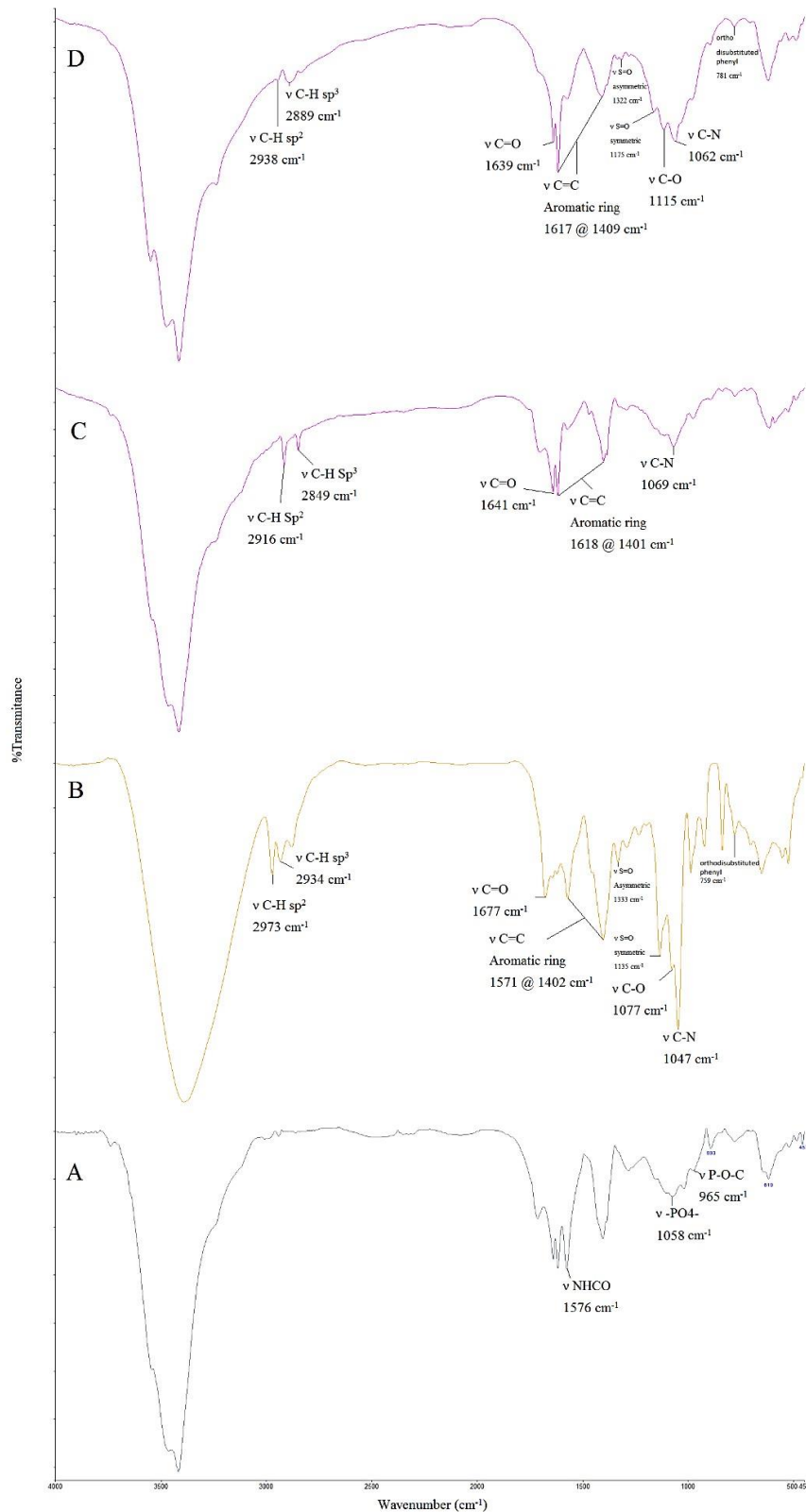


Figure 1. chitosan hydrogel (A); Gp cross-linked chitosan hydrogel (B)

At the final compound, the piroxicam-methadone group, the FTIR results (Figure 2D) showed all the indicator peaks of chitosan, GP, piroxicam, and methadone together.

This Figure (Figure 2D) confirmed the mixture of piroxicam and methadone in the crosslinked hydrogel of chitosan and GP.



**Figure 2.** FTIR spectra of chitosan (A), piroxicam (B), methadone (C), and piroxicam-methadone (D) groups

### 3.3. Hydrogel's Gelation Time

As the temperature increased from 24 to 37 °C, the solidification time of the hydrogel decreased from 35 minutes to 21 minutes. The hydrogel formulation's gelling process is temperature and time dependent; as a result, the gelation process speeds up as the temperature rises. At low temperatures, strong interactions between water molecules and chitosan prevent chitosan chains from joining together. Although the salt phosphate group's electrostatic repulsion of chitosan chains is neutralized by the addition of GP, there is still insufficient energy to overcome the solvent/polymer interaction and disturb the regular arrangement of water molecules around the chitosan chains. Such a solution can be stable for hours at room temperature. When the temperature rises, the hydrophobic interactions of chitosan-chitosan become stronger, altering the structure of water molecules that enclose the chitosan chains' shells. As the temperature rises, the hydrogen bonds between the chains get stronger, and the gelation process is completed by the chitosan chains combining.

### 3.4. In Vitro Released Piroxicam and Methadone were from the Hydrogels

Figures 3 and 4 showed that the release of piroxicam and methadone from cross-linked chitosan hydrogels follows a long-term release pattern. During the first 24 hours, chitosan hydrogel released around 82 and 87 percent of piroxicam and methadone, respectively. After 72 hours, 87% and 96% of piroxicam and methadone were released, respectively. A regression coefficient ( $r^2$ ) close to one was found to be the best strategy for determining the release kinetic pattern of piroxicam and methadone from the generated hydrogel. The values for  $r^2$  are shown in Table 1. According to the regression coefficient values, the drug release data for piroxicam hydrogel best matched Hixon crowel's kinetic model, whereas methadone hydrogel showed Higuchi's kinetic model.

### 3.5. Histopathological Examination

Histological evaluation of bone defect on the 3rd day in all groups showed an empty space with a well-defined margin. In all groups, the presence of inflammatory cells was mainly evident in

mononuclear inflammatory cells. In chitosan, piroxicam, and piroxicam-methadone groups, the number of inflammatory cells was lower than in other groups (Figure 5).

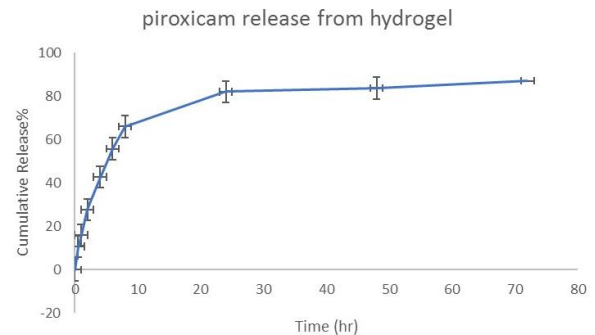


**Figure 3.** In vitro piroxicam release profile from the piroxicam group

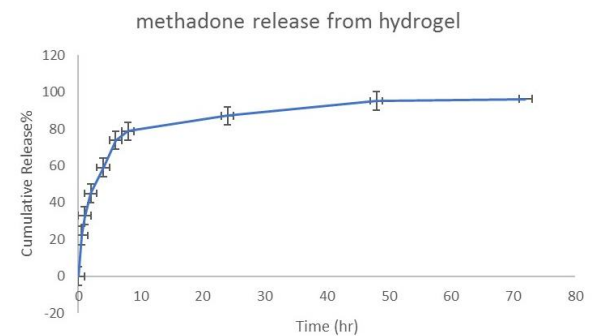


**Figure 4.** In vitro methadone release profile from the methadone group

**Table 1.** Release mathematical models' correlation coefficients of piroxicam and methadone

R <sup>2</sup> of release models	Piroxicam hydrogel	Methadone hydrogel
Zero-order	0.9184	0.8799
First-order	0.9694	0.9767
Higuchi	0.9865	0.9928
Hixon crowel	0.9927	0.9539
Krosmeier peppas	0.7635	0.8917

On the 7th day of the study, the number of inflammatory cells and the extent of bleeding at the site of the defect were lower in the three groups of piroxicam, methadone, and piroxicam-methadone groups than the other groups. Immature bone was observed as thin eosinophilic trabeculae. The formation of thin bony trabeculae had begun from the periphery to the center of the defect, and small spaces of bone marrow were also observed between them. The newly formed immature bones were covered with

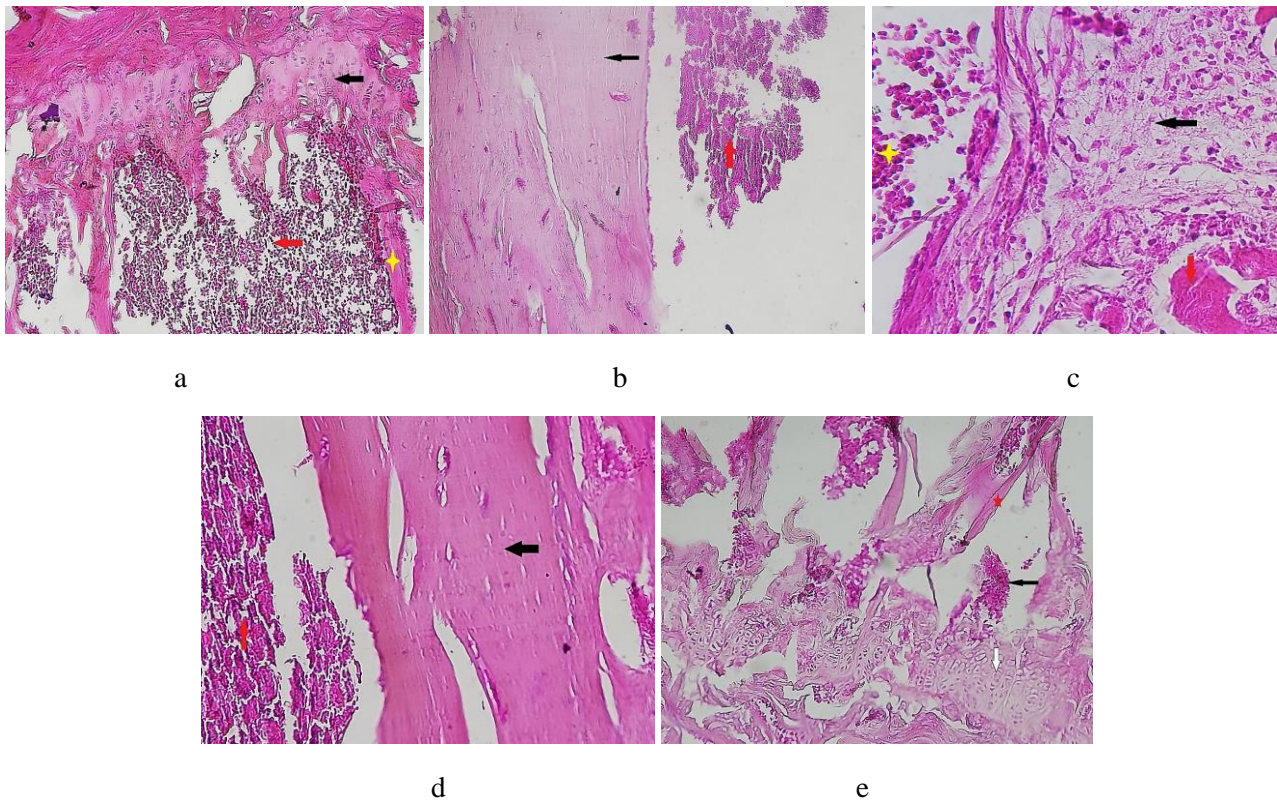


**Figure 5.** Histological section (H&E staining) of proximal tibial epiphysis defect in the control group on day 3. (a) Control group ( $\times 100$ ); inflammatory cells (red arrow); cartilage tissue (black arrow); woven bone formation (yellow star). (b) Chitosan group ( $\times 100$ ); inflammatory cells (red arrow); bone blades (black arrow). (c) Piroxicam group ( $\times 400$ ); delicate and irregular bony blades (red arrow); connective tissue (black arrow); inflammatory cells (yellow star). (d) Methadone group ( $\times 400$ ); inflammatory cells (red arrow); woven bone formation (black arrow). (e) Piroxicam-methadone group ( $\times 100$ ); inflammatory cells (black arrow); cartilage tissue (white arrow); Thin bony blades (red star)

active osteoblasts (as a sign of active osteogenesis). In the control and piroxicam-methadone groups, the number of inflammatory cells was higher and the filling of the bone defect with immature bone was minimal (Figure 6).

On day 21, there was no evidence of hemorrhage at the defect site and the number of inflammatory cells was significantly reduced in histopathological evaluation in the evaluated groups. Most of the defect was filled with newly formed bone. In tissue sections, immature bone blades were being replaced by primary lamellar bone. In the control and piroxicam-

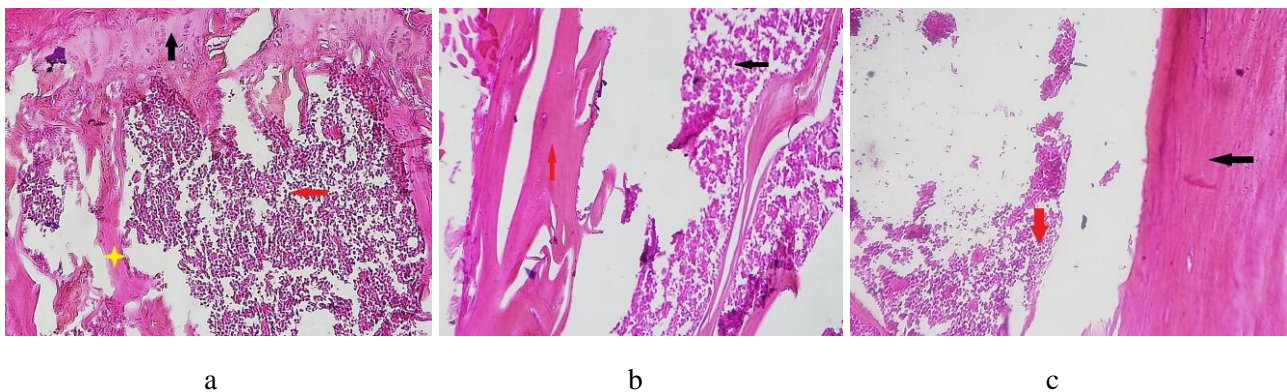


**Figure 6.** Histological section (H&E staining) of proximal tibial epiphysis defect on day 7. (a) Piroxicam group ( $\times 400$ ); Inflammatory cells (red arrow); cartilage tissue (black arrow); Thin bony blades (yellow star). (b) Methadone group ( $\times 100$ ); inflammatory cells (black arrow); irregular bone blades (red arrow). (c) Piroxicam-methadone group ( $\times 100$ ); inflammatory cells (red arrow); bone blades (black arrow)

methadone groups, the amount of bone formation was less than other groups and most of the bone tissue was still immature. Also, the bone tissue in these groups had less density and organization compared to the other groups.

Histological evaluation showed better repair in the chitosan, piroxicam, and methadone groups (Figure 7).

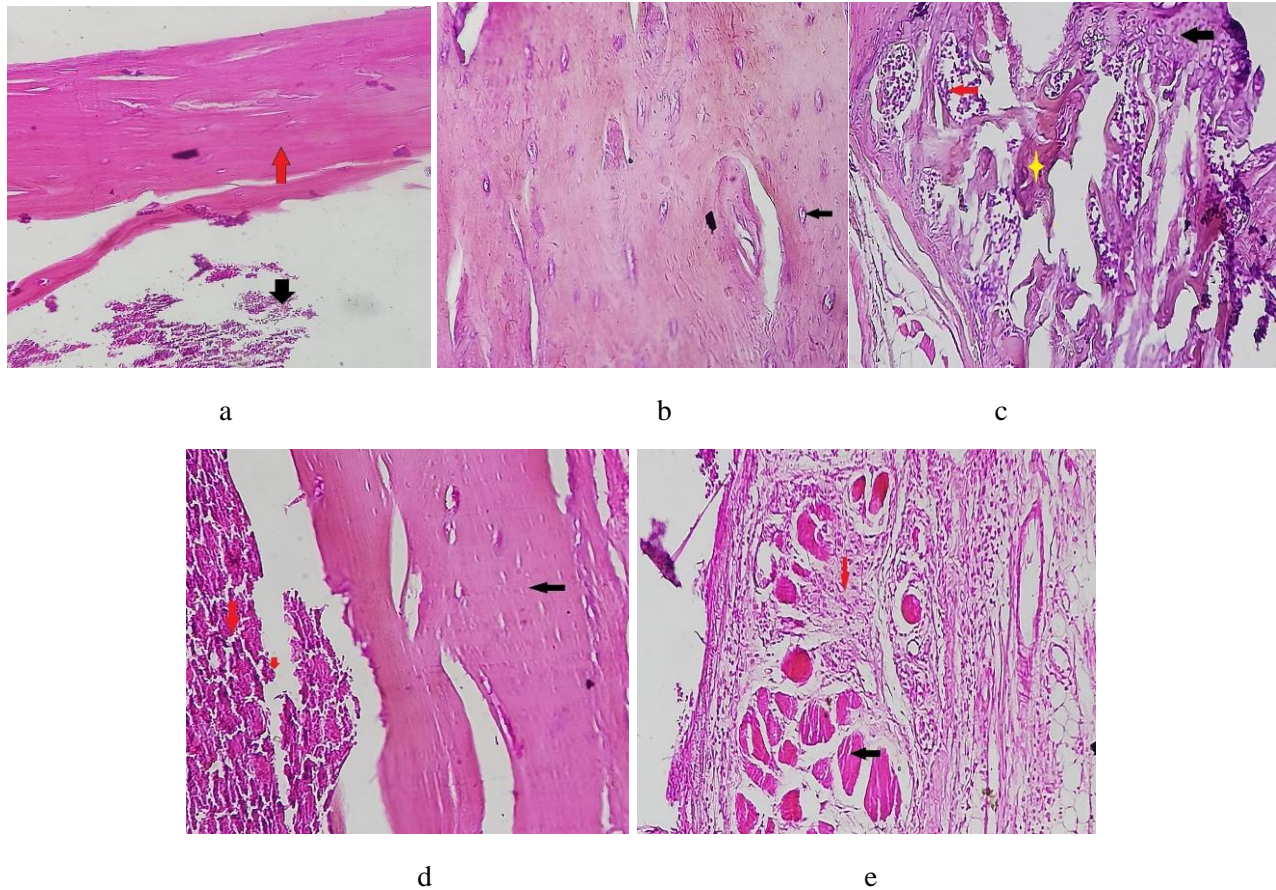


**Figure 7.** Histological section (H&E staining) of proximal tibial epiphysis defect in the control group on day 21. (a) Control group ( $\times 400$ ). Inflammatory cells (black arrow); bone blades and fusion at the site of the bone defect (red arrow). (b) Chitosan group ( $\times 400$ ); Bone blades, osteocytes, and lacunae (black arrow). (c) Piroxicam group ( $\times 100$ ); inflammatory cells (red arrow); cartilage tissue (black arrow); bone blades at the site of the bone defect (yellow star). (d) Methadone group ( $\times 400$ ); inflammatory cells (red arrow); relatively dense bone blades (black arrow). (E) Piroxicam-methadone group ( $\times 400$ ); connective tissue (red arrow); delicate and irregular bony blades (black arrow)

#### 4. Discussion

In the present study, a controlled-release drug delivery system loaded with methadone, piroxicam, and combination of piroxicam-methadone was used in the experimental model of bone defect and while evaluating the inflammatory response, the repair process in the defects was investigated. The aim of this study was to prepare a novel formulation of controlled-release hydrogel loaded with methadone and piroxicam in the experimental model of bone defect by using a well-known cross-linked chitosan hydrogel [13].

Cross-linked chitosan morphological evaluations by SEM revealed more complex networks than non-cross-linked chitosan. The slow-release drug delivery system generated this intricate network. Several researches have used this cross-linking approach in chitosan hydrogels, and similar findings in terms of the morphological structure have been produced. The structure of the piroxicam-methadone group was validated using the FTIR method, as mentioned in the Results section. The FTIR spectra of the piroxicam-methadone group were compared to that of the chitosan, methadone and piroxicam groups, among other compounds. The composite sample of the piroxicam-methadone group

was shown in Figure 2D. Figure 2 shows the findings of FTIR investigations on hydrogels, with some identified peaks being unique to each material. These findings demonstrate the presence of some trapping of substances such as chitosan, GP, piroxicam, and methadone. The final hydrogel senses both pH and temperature by adding GP solution to the chitosan solution. Strong interactions between water molecules and chitosan prohibit chitosan chains from coming together at low temperatures. As a result, a chitosan hydrogel can be stable at ambient temperature for hours. The electrostatic repulsion of chitosan chains by the salt phosphate group is neutralized by adding GP salt. The hydrogen bonds between the chains are strengthened as a result of the higher temperature, and the gelation process is eventually completed by the merging of the chitosan chains. The gelation time of the produced hydrogel was above 37°C and lasted for about 21 minutes. The gelation process was enhanced by raising the temperature from 24 to 37°C. When within the syringe, this mixture was in sol form at room temperature. After being injected into the body, the temperature is raised to 37 degrees, causing the hydrogel to gel and operate as a controlled-release system. In the current study on drug release, the pattern of release indicated 72 hours of sustained in-vitro drug release for both methadone and piroxicam formulations. In terms of drug release kinetics, the drug release from the formulation was best matched to Higuchi and Crowel's kinetic models for piroxicam and methadone hydrogel, respectively, based on regression coefficient values. These sustained-release parenteral dosage forms may be appealing to animals because they reduce the need for frequent injections, improve drug therapy compliance, and have a good pharmacokinetic profile.

It has been suggested that bone repair is highly dependent on the persistence and severity of the inflammatory phase because immune cells play an important role in bone repair modulation. Within 48 hours after the occurrence of bone injury, the inflammatory process at the site of injury reaches its maximum and is completed within 7 days [16, 17]. In fact, leukocytes are the main cellular components of inflammation and the immune response, and their penetration into the fracture hematoma following bone injury has been described as characteristic of the inflammatory phase of fracture healing [18]. Similarly, on the 3rd day of the present study, the presence of inflammatory cells, mostly mononuclear, at the fracture site was seen in all evaluated groups and descriptive

evaluation of tissue sections showed the highest inflammatory response in the control group. But on the 7th day after the injury, the number of inflammatory cells at the site of the defect was significantly lower in the piroxicam, methadone, and piroxicam-methadone groups than in the control and chitosan groups. One of the important roles of inflammatory cells is the secretion of pro-inflammatory mediators including TNF- $\alpha$ , IL-1, IL-6, and CCL2. These mediators recruit more inflammatory cells and mesenchymal cells to the site of damage [3, 19]. The production of some inflammatory cytokines has been shown to be involved in bone repair. For example, TNF- $\alpha$  stimulates osteoclastogenesis and inhibits osteoblast function [20].

In the evaluated controlled-release system, chitosan was used as a scaffold for loading piroxicam and methadone. The usefulness of chitosan in the bone repair process has already been reported [20, 21]. As a bone scaffold, chitosan supports the attachment and proliferation of bone-forming osteoblasts and is also involved in the mineralization of the bone matrix [23]. In addition, chitosan scaffolds play a role in osteoconductivity in bone defects [24]. It has been suggested that chitosan may inhibit the synthesis of some inflammatory mediators such as IL-1 $\beta$ , reduce oxidative stress metabolites, and promote some anti-inflammatory markers such as IL-10 [11]. Therefore, based on the mechanisms mentioned, it seems that the use of chitosan hydrogel as a scaffold in the drug delivery system of the present study was the right choice. This is well confirmed by less healing in the control group. But it seems that in the groups where chitosan hydrogel was also used as a scaffold, the bone repair was not the same. In fact, the difference in repair in the groups containing chitosan can be attributed to the drugs loaded on this scaffold.

With the onset of acute inflammation of tissue-resident cells, including tissue macrophages, lymphocytes, endothelial cells, fibroblasts, and mast cells, identify invasive pathogens or tissue injury byproducts and then release various pro-inflammatory mediators, including cytokines, chemokines, and growth factors [12]. In fact, leukocytes are the main cellular components of inflammation and the immune response, and their penetration into the fracture hematoma following bone injury has been described as characteristic of the inflammatory phase of fracture healing [12]. Inflammation is thought to be an important part of the fracture healing process in which the

production of prostaglandins by COX-2 is involved. Animal investigations suggest that NSAIDs, which inhibit COX-2, may impair fracture healing by inhibiting the endochondral ossification pathway. Data from animal studies suggest that NSAIDs, which inhibit COX-2, can impair fracture healing due to the inhibition of the endochondral ossification pathway [25]. But it is better to say that long-term or high dose administration of NSAIDs for the management of fracture pain can interfere with osteogenesis and increase the risk of nonunion [26-28].

Consistent with the previous contradictory results, the histological results of the present study also showed that piroxicam used in the controlled release system of the present study did not have an adverse effect on bone repair and reduced local inflammation and controlled the presence of inflammatory cells at the fracture site after the administration of chitosan hydrogels loaded with piroxicam was seen.

It has been shown that opioids in humans can induce immune suppression and control the release of inflammatory substances [29, 30]. Opioids have been shown to have a negative effect on bone healing. However, it should be noted that the clinical data related to this claim are about opioid users and long-term opioid treatment [31, 32]. In addition, it is stated that not all opioids have a negative impact on bone repair. Interestingly, Methadone is one of the opiates that does not impair bone healing [31]. The analgesic effect of methadone in canine orthopedic surgery has been well demonstrated [33]. Therefore, methadone by providing sedation and analgesia after bone injury and due to control of postoperative inflammation [33] can play a positive role in the healing of bone fractures and this conclusion is in agreement with the results of the present study.

The point to be considered is why the bone healing in the piroxicam-methadone group was similar to the healing in the control group and less than the other treatment groups. Has the presence of methadone and piroxicam in the chitosan scaffold, which itself has anti-inflammatory effects, resulted in this negative effect due to excessive suppression of inflammation? This is a question and a concept that needs further investigation. In fact, the inflammatory phase is an important component of healing, and ultimately healing can be affected by the severity and extent of post-fracture injury, damage to the soft tissues adjacent to the fracture, and

therapeutic interventions. It is clear that therapeutic interventions affect bone repair by intervening in various factors, especially inflammatory responses. In other words, just as the removal of the inflammatory phase can impair healing, sometimes with therapeutic interventions due to the limited control of excessive inflammation caused by injury and fracture, it is necessary to accelerate bone healing at the same time as providing pain relief to the patient.

## 5. Conclusion

In the present study, histological examination of bone defects on the 3rd day of the study in all groups showed that mononuclear inflammatory cells were the most common type of inflammatory cells. At this time, in the chitosan, piroxicam, and piroxicam-methadone groups, the number of inflammatory cells was lower than in other groups. On the 7th day of the study, the number of inflammatory cells and the extent of bleeding at the site of the defect were lower in the three groups of piroxicam, methadone, and piroxicam-methadone than the other groups. In the control group, the number of inflammatory cells was higher and the filling of the bone defect with immature bone was minimal. On day 21, the number of inflammatory cells was significantly reduced in histopathological evaluation in all evaluated groups. Most of the defect was filled with newly formed bone. Histological evaluation showed better repair in the chitosan, piroxicam, and methadone groups. In fact, by microscopic evaluation of the tissue sections, it revealed moderate inflammation control and better repair in the groups of chitosan, piroxicam, and methadone. It seems that in the control group that did not receive any treatment intervention, following the experimental bone defect, the highest inflammatory response was observed in histological examination and finally the weakest bone repair. On the other hand, the presence of piroxicam, methadone, and chitosan in the piroxicam-methadone group (all of which have anti-inflammatory effects) also seems to have a negative effect on the repair.

## Acknowledgments

The present study has been approved by the Research Council of the Faculty of Veterinary Medicine at Shahrekord University [1399-08-07].

## References

- 1- Paschalia M Mountziaris and Antonios G Mikos, "Modulation of the inflammatory response for enhanced bone tissue regeneration." *Tissue Engineering Part B: Reviews*, Vol. 14 (No. 2), pp. 179-86, (2008).
- 2- Tamiyo Kon *et al.*, "Expression of osteoprotegerin, receptor activator of NF- $\kappa$ B ligand (osteoprotegerin ligand) and related proinflammatory cytokines during fracture healing." *Journal of Bone and Mineral Research*, Vol. 16 (No. 6), pp. 1004-14, (2001).
- 3- Florence Loi, Luis A Córdova, Jukka Pajarinen, Tzu-hua Lin, Zhenyu Yao, and Stuart B Goodman, "Inflammation, fracture and bone repair." *Bone*, Vol. 86pp. 119-30, (2016).
- 4- YM Kuang, YC Zhu, Ying Kuang, Yuan Sun, Chen Hua, and WY He, "Changes of the immune cells, cytokines and growth hormone in teenager drug addicts." *Xi bao yu fen zi Mian yi xue za zhi= Chinese Journal of Cellular and Molecular Immunology*, Vol. 23 (No. 9), pp. 821-23, (2007).
- 5- Alexander Beck, Khaled Salem, Gert Krischak, Lothar Kinzl, Mark Bischoff, and Andreas Schmelz, "Nonsteroidal anti-inflammatory drugs (NSAIDs) in the perioperative phase in traumatology and orthopedics effects on bone healing." *Operative Orthopädie und Traumatologie*, Vol. 17 (No. 6), pp. 569-78, (2005).
- 6- Anneluuk LC Lindenhovious, Gijs TT Helmerhorts, Alexandra C Schnellen, Mark Vrahas, David Ring, and Peter Kloen, "Differences in prescription of narcotic pain medication after operative treatment of hip and ankle fractures in the United States and The Netherlands." *Journal of Trauma and Acute Care Surgery*, Vol. 67 (No. 1), pp. 160-64, (2009).
- 7- Javad Parvizi and Michael R Bloomfield, "Multimodal pain management in orthopedics: implications for joint arthroplasty surgery." *Orthopedics*, Vol. 36 (No. 2), pp. 7-14, (2013).
- 8- Ippokratis Pountos, Theodora Georgouli, Giorgio M Calori, and Peter V Giannoudis, "Do nonsteroidal anti-inflammatory drugs affect bone healing? A critical analysis." *The Scientific World Journal*, Vol. 2012(2012).
- 9- Xiangjun Kong, Jing Wang, Lingyan Cao, Yuanman Yu, and Changsheng Liu, "Enhanced osteogenesis of bone morphology protein-2 in 2-N, 6-O-sulfated chitosan immobilized PLGA scaffolds." *Colloids and Surfaces B: Biointerfaces*, Vol. 122pp. 359-67, (2014).
- 10- Marcelino Montiel-Herrera *et al.*, "N-(furfural) chitosan hydrogels based on Diels–Alder cycloadditions and application as microspheres for controlled drug release." *Carbohydrate polymers*, Vol. 128pp. 220-27, (2015).
- 11- Abolfazl Barzegar and Moosa Javdani, "Application of chitosan hydrogels in traumatic spinal cord injury; a therapeutic approach based on the anti-inflammatory and antioxidant properties of selenium nanoparticles." *Frontiers in Biomedical Technologies*, (2022).
- 12- Marcelino Montiel-Herrera *et al.*, "N-(furfural) chitosan hydrogels based on Diels–Alder cycloadditions and application as microspheres for controlled drug release." *Carbohydrate polymers*, Vol. 128pp. 220-27, (2015).
- 13- Oluwadamilola M Kolawole, Wing Man Lau, and Vitaliy V Khutoryanskiy, "Chitosan/ $\beta$ -glycerophosphate in situ gelling mucoadhesive systems for intravesical delivery of mitomycin-C." *International Journal of Pharmaceutics: X*, Vol. 1p. 100007, (2019).
- 14- Moosa Javdani, Farid Shahbandari, Ehsan Soleymanijadian, Mohammad Hashemnia, and Abolfazl Barzegar, "Induction of Experimental Endometriosis in Rat: Evaluation of Systemic Inflammatory Response and Liver Tissue Changes." *Tabari Biomedical Student Research Journal*, Vol. 4 (No. 4), pp. 1-12, (2022).
- 15- Moosa Javdani, Maryam Nafar, Abdolnaser Mohebi, Pegah Khosravian, and Abolfazl Barzegar, "Evaluation of Leukocyte Response due to Implant of a Controlled Released Drug Delivery System of Chitosan Hydrogel Loaded with Selenium Nanoparticle in Rats with Experimental Spinal Cord Injury." *Tabari Biomedical Student Research Journal*, Vol. 4 (No. 2), pp. 1-16, (2022).
- 16- Tae-Joon Cho, Louis C Gerstenfeld, and Thomas A Einhorn, "Differential temporal expression of members of the transforming growth factor  $\beta$  superfamily during murine fracture healing." *Journal of bone and mineral research*, Vol. 17 (No. 3), pp. 513-20, (2002).
- 17- Rozalia Dimitriou, Eleftherios Tsiridis, and Peter V Giannoudis, "Current concepts of molecular aspects of bone healing." *Injury*, Vol. 36 (No. 12), pp. 1392-404, (2005).
- 18- Lutz Claes, Stefan Recknagel, and Anita Ignatius, "Fracture healing under healthy and inflammatory conditions." *Nature Reviews Rheumatology*, Vol. 8 (No. 3), pp. 133-43, (2012).
- 19- Jukka Pajarinen *et al.*, "Mesenchymal stem cell-macrophage crosstalk and bone healing." *Biomaterials*, Vol. 196pp. 80-89, (2019).
- 20- Bilal Osta, Giulia Benedetti, and Pierre Miossec, "Classical and paradoxical effects of TNF- $\alpha$  on bone homeostasis." *Frontiers in immunology*, Vol. 5p. 48, (2014).
- 21- Sheeny K Lan Levengood and Miqin Zhang, "Chitosan-based scaffolds for bone tissue engineering." *Journal of Materials Chemistry B*, Vol. 2 (No. 21), pp. 3161-84, (2014).
- 22- Jayachandran Venkatesan and Se-Kwon Kim, "Chitosan composites for bone tissue engineering—an overview." *Marine drugs*, Vol. 8 (No. 8), pp. 2252-66, (2010).

- 23- Yang-Jo Seol *et al.*, "Chitosan sponges as tissue engineering scaffolds for bone formation." *Biotechnology letters*, Vol. 26 (No. 13), pp. 1037-41, (2004).
- 24- RAA Muzzarelli *et al.*, "Stimulatory effect on bone formation exerted by a modified chitosan." *Biomaterials*, Vol. 15 (No. 13), pp. 1075-81, (1994).
- 25- Piet Geusens, Pieter J Emans, Joost JA de Jong, and Joop van den Bergh, "NSAIDs and fracture healing." *Current opinion in rheumatology*, Vol. 25 (No. 4), pp. 524-31, (2013).
- 26- Alexander Beck, Khaled Salem, Gert Krischak, Lothar Kinzl, Mark Bischoff, and Andreas Schmelz, "Nonsteroidal anti-inflammatory drugs (NSAIDs) in the perioperative phase in traumatology and orthopedics effects on bone healing." *Operative Orthopadie und Traumatologie*, Vol. 17 (No. 6), pp. 569-78, (2005).
- 27- Christopher J Richards, Kenneth W Graf, and Rakesh P Mashru, "The effect of opioids, alcohol, and nonsteroidal anti-inflammatory drugs on fracture union." *Orthopedic Clinics*, Vol. 48 (No. 4), pp. 433-43, (2017).
- 28- Robert W van Esch, Maurice M Kool, and Saskia van As, "NSAIDs can have adverse effects on bone healing." *Medical hypotheses*, Vol. 81 (No. 2), pp. 343-46, (2013).
- 29- J David Clark *et al.*, "Morphine reduces local cytokine expression and neutrophil infiltration after incision." *Molecular pain*, Vol. 3pp. 1744-8069-3-28, (2007).
- 30- Yong-min Liu, Sheng-mei Zhu, Kui-rong Wang, Zhi-ying Feng, and Qing-lian Chen, "Effect of tramadol on immune responses and nociceptive thresholds in a rat model of incisional pain." *Journal of Zhejiang University SCIENCE B*, Vol. 9 (No. 11), pp. 895-902, (2008).
- 31- Flaminia Coluzzi, Maria Sole Scerpa, and Marco Centanni, "The effect of opiates on bone formation and bone healing." *Current Osteoporosis Reports*, Vol. 18 (No. 3), pp. 325-35, (2020).
- 32- Alexander Beck, Khaled Salem, Gert Krischak, Lothar Kinzl, Mark Bischoff, and Andreas Schmelz, "Nonsteroidal anti-inflammatory drugs (NSAIDs) in the perioperative phase in traumatology and orthopedics effects on bone healing." *Operative Orthopadie und Traumatologie*, Vol. 17 (No. 6), pp. 569-78, (2005).
- 33- Larissa B Cardozo *et al.*, "Evaluation of the effects of methadone and tramadol on postoperative analgesia and serum interleukin-6 in dogs undergoing orthopaedic surgery." *BMC veterinary research*, Vol. 10 (No. 1), pp. 1-7, (2014).